Title
EXPERIMENTAL STUDY OF SELF-FOCUSING IN A LIQUID CRYSTALLINE MEDIUM

Author
Hanson, E.G.

Publication Date
1976-12-01

Submitted to Applied Physics

LBL-6084
Preprint

EXPERIMENTAL STUDY OF SELF-FOCUSING IN A LIQUID CRYSTALLINE MEDIUM

E. G. Hanson, Y. R. Shen, and G. K. L. Wong

December 1976

Prepared for the U. S. Energy Research and Development Administration under Contract W-7405-ENG-48

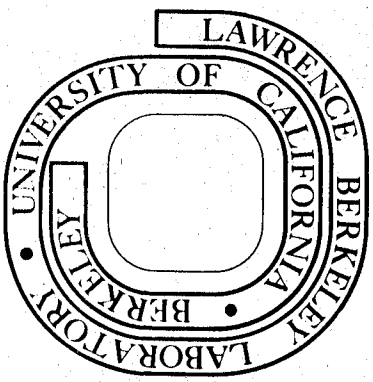

DISCLAIMER

Submitted to Applied Physics

LBL-6084

EXPERIMENTAL STUDY OF SELF-FOCUSING IN A LIQUID CRYSTALLINE MEDIUM*

E. G. Hanson, Y. R. Shen, and G. K. L. Wong

DECEMBER 1976

*Supported by the National Science Foundation Grant No. DMR 76-19843.

EXPERIMENTAL STUDY OF SELF-FOCUSING IN A LIQUID CRYSTALLINE MEDIUM*

E. G. Hanson and Y. R. Shen

Physics Department, University of California
Berkeley, California 94720

and

G. K. L. Wong

Physics Department, Northwestern University
Evanston, Illinois 60201

DECEMBER 1976

ABSTRACT

We have studied experimentally self-focusing of light in the liquid crystalline medium p-ethoxybenzyldine-p-butylaniline (EBBA). By variation of temperature, the response time of the field-induced refractive index was adjusted from larger than to smaller than the Q-switched laser pulsewidth. Accordingly, self-focusing varied from transient to quasi-steady-state. The results agree well with existing theoretical predictions and can be qualitatively understood from a simple physical description. The induced stimulated Brillouin scattering was also measured and was shown to be responsible for the limiting diameter of the self-focused beam in the present case.

---

*Supported by the National Science Foundation Grant No. DMR 76-19843.

I. INTRODUCTION

Self-focusing of light is one of the most complex and interesting phenomena in nonlinear optics.[1] It is of central importance in the design of high-power laser amplifiers because of its role in possible laser-induced damages. It is of fundamental interest as well because of its interplay with many other nonlinear optical processes.

While many physical aspects of self-focusing are now well understood, a number of important questions still remain, namely, the detailed dynamics of focusing, the limiting focusing diameter, polarization properties, etc. In particular, it is not clear how the self-focusing behavior changes in accordance with the variation in the laser pulsewidth t_p, relative to the response time τ of the induced refractive index in the medium.

When $t_p \gg \tau$, in the so-called quasi-steady-state limit, the moving focus model[2] describes the self-focusing behavior very well. This model was first suggested by Lugovoi and co-workers,[3] who realized that a self-focused beam leads to one or more sharp focal spots which move along the beam axis as the beam power varies during a laser pulse. The model actually follows closely the earlier theoretical calculation of steady-state self-focusing. Experiments performed with well-controlled, single transverse mode lasers have confirmed the predictions of the calculations. The motion of the focal spot has been observed by time of flight measurements,[4,5] and has been photographed directly with a streak camera.[6] It explains the observed backward-forward asymmetry in stimulated Raman scattering[7,8] and the time dependence of the stimulated Raman and Brillouin

pulses under various self-focusing conditions.[8,9] In addition, it explains quantitatively the spectral broadening of the self-focused beam resulting from self-phase modulation.[10,11] Measurements of the self-focusing dynamics in the prefocal region[12] also agree well with the theoretical calculations.[13,14]

When $\tau >> t_p$, transient response of the medium dominates the self-focusing behavior. Focusing becomes much more gradual and no sharp focal spot is formed. Transient self-focusing was first discussed by Akhmanov et al.[15] It was shown that as the laser pulse propagates on in the nonlinear medium, the beam radius would first deform into a horn shape (see Sec. II B) and then retains the shape over long distances. This is known as dynamic trapping. Numerical calculations yield this same picture,[16-18] although they suggested that the neck of the horn might continue to shrink in radius as the pulse propagates on and may even form singularities.[19] This dynamic trapping model of transient self-focusing has been used to semi-quantitatively account for the observed asymmetric semi-periodic spectral broadening of the laser light.[8,20] Experiments using an isotropic liquid crystalline material with a long relaxation time τ as the nonlinear medium have been performed to study this extreme transient self-focusing [21] and have confirmed the theoretical predictions. It has been shown that the pulse does deform into a horn shape. The diameter of the neck of the horn first decreases almost exponentially with increasing input power, as predicted,[18] and then approaches a constant when some limiting nonlinear process sets in.

As is described above, the dynamic trapping model for transient self-focusing ($t_p << \tau$), and the moving focus model for quasi-steady-state self-focusing, ($t_p >> \tau$) appear to be very different physically. It is

therefore interesting to know how self-focusing would vary as t_p/τ is varied from one limit to the other. This has not been studied either experimentally or theoretically. Experimentally, difficulty comes in the choice of a suitable nonlinear medium with τ variable over a wide range or a laser with a variable t_p. While the former seems easier, in order to quantitatively measure the time dependence of the focusing, a laser pulse with t_p of the order of 10 nsec or longer must be used, as limited by the response time of ordinary detection systems. These constraints rule out the use of conventional Kerr liquids, for which τ is in the 1-100 psec range.

We have found recently that a nematic liquid crystal in the isotropic phase can have a τ variable from $\sim$ 1 nsec to > 100 nsec depending on the temperature.[22,23] Such a medium also has a large nonlinearity in which self-focusing of a Q-switched laser pulse readily occurs. We therefore have on hand a perfect medium we can use to study the entire range of self-focusing from the quasi-steady-state to the transient limit. In this paper, we discuss in quantitative detail our recent measurements of self-focusing in a liquid crystalline medium with t_p/τ varied from $<< 1$ to $>> 1$.

Section 2 gives a brief review of the theory and physical description of self-focusing under different conditions. Section 3 summarizes our experimental techniques, data analysis and results. Section 4 shows how our experimental results agree with a qualitative united physical description of self-focusing in all cases. We also identify the mechanism responsible for the limiting focal diameter in our sample.

II. THEORY

A. General Formalism

Consider a medium with a refractive index $n = n_o + \delta n(|E|^2)$, where δn is the part induced by the optical field E. This induced δn leads to self-focusing which is governed by the wave equation[1]

$$\nabla^2 E - \frac{1}{c^2}\frac{\partial^2}{\partial t^2}[(n_o + \delta n)E] = 0. \tag{1}$$

For a quasi-monochromatic light beam we can write

$$E = A(r,z,\zeta)\exp[ikz - i\omega t + iks(r,z,\zeta)] \tag{2}$$

where $\zeta \equiv t - zn_o/c$ is the reduced time, and A and s are respectively the amplitude and the eikonal (or phase function) of the wave. We can convert Eq. (1) into two coupled equations

$$\frac{\partial A}{\partial z} + \left(\frac{\partial s}{\partial r}\right)\left(\frac{\partial A}{\partial r}\right) + \frac{A}{2}\left(\frac{\partial^2 s}{\partial r^2} + \frac{1}{r}\frac{\partial s}{\partial r}\right) = 0 \tag{3a}$$

$$2k\left(\frac{\partial s}{\partial z}\right) + \left(\frac{\partial s}{\partial r}\right)^2 = 2\frac{\delta n}{n_o} + \frac{1}{A}\left(\frac{\partial^2 A}{\partial r^2} + \frac{1}{r}\frac{\partial A}{\partial r}\right). \tag{3b}$$

In order to solve these equations, we need to know the amplitude and phase profile of the input laser pulse. We also need to know the functional dependence of δn upon the field. For Kerr liquids, the dominant mechanism contributing to δn is molecular reorientation.[15,22-24] It obeys a relaxation equation

$$\left[1 + \tau\frac{\partial}{\partial t}\right]\delta n = n_2|E|^2, \tag{4}$$

which yields

$$\delta n(t) = \frac{n_2}{\tau} \int_{-\infty}^{t} |E(t')|^2 \, e^{-(t - t')/\tau} \, dt, \tag{5}$$

where n_2 is a constant coefficient of the medium. Then, in the quasi-steady-state limit ($t_p >> \tau$),

$$\delta n(t) = n_2 |E(t)|^2, \tag{6}$$

and, in the extreme transient limit ($t_p << \tau$),

$$\delta n(t) = \frac{n_2}{\tau} \int_{-\infty}^{t} |E(t')|^2 \, dt'. \tag{7}$$

Self-focusing can now be described by the solution of the coupled equations in Eq. (3) together with Eq. (5). Unfortunately, an analytical solution is not generally possible, so these equations have been solved numerically. In the quasi-steady-state limit, the calculation predicts the appearance of a sharp focal spot at the self-focusing distance[14]

$$z_f(\zeta) = \frac{K}{\sqrt{P(\zeta)} - 0.858 \sqrt{P_{cr}}}, \tag{8}$$

$$P_{cr} = \frac{(1.22\lambda_o)^2 c_o}{128 n_2}, \tag{9}$$

where P is the input laser power, λ_o and c_o are the wavelength and the speed of light in vacuum, $K = 0.369\ ka^2\sqrt{P_{cr}}$, $k = \omega n_o/c$, and a is the input beam radius. The axial intensity of the self-focused beam is given approximately by

$$I_{ax}(z,\zeta) = I_{ax}(0,\zeta)\left[1 - (z/z_f(\zeta))^2\right]^{-\alpha/2}, \tag{10}$$

where α is a parameter which depends upon P/P_{cr}.

For the transient case, we can discuss self-focusing using the paraxial approximation. The beam is assumed to have a Gaussian transverse profile and the wavefronts are assumed to be paraboloids[1]

$$A^2(\zeta,r,z) = \frac{A_o^2(z=0,\zeta)}{f^2(z,\zeta)} e^{-(r^2/a^2f^2(z,\zeta))}$$
$$s(\zeta,r,z) = \phi(\zeta,z) + \frac{1}{2}\beta(z,\zeta)r^2 \tag{11}$$

where $f(z,\zeta) = r_o(z,\zeta)/r_o(z=0,\zeta)$ is the reduced dimensionless radius. From Eqs. (3), (5), and (11), we obtain[15]

$$\frac{1}{f}\frac{\partial^2 f(\zeta)}{\partial z^2} = \frac{1}{k^2a^4f^4(\zeta)} - \frac{n_2}{n_o a^2}\frac{1}{\tau}\int_o^\zeta \frac{A_o^2(\eta)}{f^4(\eta)} e^{(\eta-\zeta)/\tau}\, d\eta \tag{12a}$$

$$\frac{1}{f}\frac{\partial f}{\partial z}(\zeta) = \beta(\zeta) \tag{12b}$$

$$\frac{\partial\phi(\zeta)}{\partial z} = -\frac{1}{k^2a^2f^2(\zeta)} + \frac{n_2}{2n_o}\frac{1}{\tau}\int_o^\zeta \frac{A_o^2(\eta)}{f^2(\eta)} e^{(\eta-\zeta)/\tau}\, d\eta. \tag{12c}$$

In Eq. (12a), the first term on the right comes from linear diffraction, while the second term is due to self-focusing. In the transient limit, the integral in the second term builds up gradually with time. During the very first part of the pulse, it is so small that the pulse propagation is dominated by linear diffraction. In later parts of the pulse, the integral becomes larger and $\partial^2 f/\partial z^2$ becomes negative. This causes $\partial f(\zeta)/f(\zeta)\partial z$ to become negative, and the beam radius shrinks as the beam

propagates on. Towards the end of the pulse, the integral approaches a limiting value, while the linear diffraction term becomes stronger as the propagating beam shrinks in radius. After a certain propagation distance, $\partial f/fdz$ becomes less and less negative and the radius f approaches a minimum value. Thus, the longitudinal spatial profile of the pulse gets deformed into a horn shape as shown in Fig. 1c. The horn-shaped pulse then travels on without appreciable change over approximately a diffraction length $z_d = ka^2$. From Eqs. (11) and (12b), we see that the eikonal should be independent of r in the neck of the horn, where f = constant. This has in fact been observed experimentally.[20] Also, in the transient limit ($t_p \ll \tau$), Eq. (12) predicts that self-focusing will remain unchanged if n_2/τ remains constant.

The paraxial approximation of Eqs. (11) and (12) does not successfully explain the detailed transient self-focusing behavior. To obtain more exact predictions, Eqs. (3) and (5) have been solved numerically for certain input conditions.[17,20,21] Numerical calculations[16-18] show that aberrations in self-focusing are significant. They also predict that the pulse is deformed into an overall horn shape but with weak oscillation in the beam radius along the neck. Aside from the oscillation, the neck radius r_o^{min}, should remain nearly constant as the pulse propagates over a distance $z \ll z_d$, but r_o^{min} is supposed to be a strong function of P/P_{cr} and t_p/τ.

B. Physical Description

We have so far described self-focusing in the quasi-steady-state limit and in the transient limit in rather different physical terms. However, in varying from one limit to the other, we should expect the self-focusing behavior to change continuously. We therefore need a unified

physical description to describe self-focusing throughout the entire range.

In our unified description, we concentrate on how the beam radius of different parts of the laser pulse varies as a function of distance as the pulse propagates in the medium. In the quasi-steady-state limit, self-focusing and subsequent diffraction are both abrupt. Thus, each small section of the incoming laser pulse self-focuses into a sharp focal spot at the self-focusing distance z_f given by Eq. (5). We can then sketch in Fig. (1a) the evolution of the beam radius and hence the longitudinal pulse profile along the cell. The pulse enters the sample from the left. The radius of each consecutive section of the pulse (A - A, B - B, etc.) follows a different trajectory and reaches a sharp minimum at $z_f(P)$ according to its instantaneous power $P(\zeta)$. For $\ell > (z_f)_{min}$, there should be two focal spots simultaneously present on the beam axis. In practice, the second focal spot is usually prevented from forming by depletion of incoming laser power by backward stimulated Raman and Brillouin scattering initiated earlier by the first focal spot.[8] We expect the longitudinal dimension of the focal spot to be about $\Delta\zeta = \tau$.

We can similarly sketch the evolution of the beam radius and longitudinal pulse profile for the transient limit. Note however that self-focusing is now much more gradual and diffraction extremely slow because of the transient response of the medium. According to the description in Sec. II A, the front part of the pulse hardly self-focuses while the lagging part of the pulse self-focuses gradually to a limiting diameter. Then as shown in Fig. 1c, the incoming pulse first gets deformed into a horn shape and then propagates on without much further change.

Now, for the intermediate range of self-focusing, we should expect

the self-focusing and diffraction trajectory to be intermediate between the two limiting cases. Both self-focusing and diffraction are less abrupt than the quasi-steady-state case but also less gradual then the transient limiting case. The middle part of the pulse sees the largest Δn and self-focuses most strongly, while both the front and the lagging parts of the pulse do not self-focus very much. Following the above description for the beam trajectory of different parts of the laser pulse, we can then sketch again the evolution of the pulse profile for the intermediate case as shown in Fig. 1b. The sketches in Fig. 1 show that the evolution of the pulse profile will indeed change continuously as self-focusing is varied from the quasi-steady-state to the transient limit.

C. Effect of Other Nonlinear Processes on the Limiting Diameter

As the input laser power is increased, the theories discussed in Section 2 A would predict that the minimum diameter of the self-focused beam should continually become smaller. Experiments however find a limiting diameter which appears to be a characteristic of the nonlinear medium.[1]

Numerous explanations have been proposed for this limiting diameter.[14,25-32] They generally assume either saturation of Δn or depletion of the laser beam.[1] While the pre-breakdown ionization[29] which creates free electrons to reduce Δn may be the domination mechanism for limiting the focal diameter in self-focusing of picosecond pulses, stimulated Raman and Brillouin scattering appears to be the most possible mechanism for the cases of longer pulses. A large fraction of the incoming laser power can be depleted by stimulated Raman and Brillouin scattering during self-focusing so that the self-focusing strength is limited. The limiting focal diameter is presumably the result of balancing between in-

crease of stimulated scattering gain due to self-focusing and decrease of self-focusing strength due to depletion of laser power by stimulated scattering. Rehn and Maier[32] have considered the possibility of forward stimulated Raman scattering as the mechanism for the limiting diameter. Kelley and Gustafson[31] have considered backward stimulated scattering. However, in either case, no serious calculation in connection with the real physical problems has been carried out.

III. EXPERIMENT

Our experiment was designed to check the predictions of the unified physical description of self-focusing discussed in the previous section. We wanted to obtain the results quantitatively so that the data can be used to compare with available or possible numerical calculations.

We used the response time τ of the medium as a varying parameter to vary self-focusing from the quasi-steady-state limit to the transient limit. In order to compare our results with the sketches in Fig. 1, we should have measured the beam radius $r_o(z,\zeta)$ defined, for example, as

$$r_o(z,\zeta) = \left[P(\zeta)/\pi\, I_{ax}(z,\zeta)\right]^{\frac{1}{2}} \tag{13}$$

for a given input laser pulse of power $P(t)$. (For a Gaussian beam, $r_o(z,\zeta)$ defined in Eq. (3) is the beam radius at the 1/e points.) However, this is not practically feasible. Instead, we varied the input peak power P_o and measured $r_o(z = \ell,\zeta)$ at the end of the sample. Examination of the self-focusing equation in Sec. II A shows that the evolution of $r_o(z = \ell,\zeta)$ with increasing peak input power should appear qualitatively the same as the evolution of $r_o(z,\zeta)$ along z with constant P_o.

A. The Nonlinear Medium

We used the liquid crystalline material p-ethoxy-benzylidene-p-butylaniline (EBBA) in its isotropic liquid phase as our self-focusing medium. This material is known to have a large nonlinear refractive index and a long relaxation time.[22] In addition, both n_2 and τ have a strong pretransitional temperature dependence in the range above the nematic-isotropic transition temperature T_K. They can be written as[22]

$$n_2 = \frac{6.35 \times 10^{-9} \text{ esu } °K}{(T - T^*)}$$

$$\tau = \frac{e^{2800° \text{ K}/T} \; 7.0 \times 10^{-11} \text{nsec} - °K}{(T - T^*)} \qquad (14)$$

where $T^* = T_K - 1.0°$ K is a ficticious second-order transition temperature. Over the temperature range we used, n_2 varied by a factor of 20, while τ varied by a factor of 50 (see Table I).

We used in our self-focusing experiment EBBA purchased from Varilight Corporation without further purification. The sample was placed in a 10-cm fused-quartz optical cell, and evacuated for several hours to remove any H_2O or O_2. After evacuation, the cell was sealed under vacuum. The sample then had a sharp isotropic-nematic transition at $T_K = 78.0°$ C. This T_K was constant to within 0.1° C throughout the experiment, indicating that no degradation of the sample had occured. In our experiment, the sample cell was held inside an oven which had a temperature stability of better than 0.1° C, and a uniformity of better than 0.2° C throughout the cell.

B. Experimental Technique

These experiments were performed with a ruby laser, Q-switched by cryptocyanine in methanol, which gave a smooth output pulse having a dur-

ation approximately 15 nsec full width at half maximum. Oscillation on a single transverse mode was insured by placing an 0.8 mm diameter pinhole in the laser cavity. The laser power was varied using neutral density filters outside the cavity. After collimation by lenses L1 and L2 (see Fig. 2) the beam entered the sample with a 1/e intensity radius of 130 μm. The time dependence of the input power was monitored by D2 (ITT-F4018 bi-planar vacuum photodiode) and by Scope A (Tek. 519).

After the beam excited the sample cell, measurements were made on it to observe the effects of self-focusing. First, a magnified image of the exit plane of the sample was formed using imaging lenses, and the actual measurements were performed on the magnified image. An image of any plane inside the sample would be distorted by gradients in Δn inside the sample. This is the reason we made all measurements z = constant.

To obtain the most complete information, we made three different measurements simultaneously, each using a separate magnified image of the exit plane of the sample. The first image was formed on a ground glass plane by light passing through lenses L3 and L4. This image had a magnification of 85 × and a resolution corresponding to 5 μm in the exit plane of the sample. This image was photographed with the streak camera (TRW model 1D Image Converter Camera, with model 7B streaking plug-in) at a streak rate of 1 ns/mm. The camera magnification was 0.5 ×. The camera was triggered by an electrical pulse from D - 1 (ITT-F4000 photodiode). Because of the triggering delay of the streak camera electronics, a fixed optical delay line (27.5 meters) was used before the streak camera. The reference monitor pulse from the streaking plug-in was displayed on scope A to monitor the exact time delay before initiation of the streak for each laser shot. This was necessary, as the jitter in the triggering time was

of the order of 10 nsec.

The second image was formed on the plane of the pinhole P1 with light reflected by beamsplitter B4 (reflectivity = 50%). This image, formed by lenses L3 and L5, had a magnification of 71 × and a resolution of better than 5 μm in the exit plane of the sample. The image was centered on the 0.5 mm diameter pinhole, so that light which passed through the pinhole originated in a 7 μm diameter region centered on the beam axis in the exit plane of the sample. This light was detected by D4 (ITT-F4018 photodiode) and displayed on Scope B (Tek 7904, with 7B92 time base and 7A19 vertical amplifier). This oscilloscope was triggered externally by the trigger output pulse from Scope A. In this way, the absolute time delay between signals on Scope A and Scope B could be compared.

The third image (magnification also equal to 71 ×) was formed on the film plane of a camera to monitor the time-integrated laser intensity in the exit plane of the sample. The light for this image was reflected by B4 and B5 (reflectivity = 30%).

Photodiode D3 (ITT-FW114A) monitored the presence of any backward stimulated Brillouin light. Aperture A1 blocked specular reflections from the sample cell windows because the input ruby beam entered the cell at a slight angle to the window normal. A coaxial delay cable delayed the signal from D3 so it appeared after the signal from D4 on Scope B.

C. Data Analysis

To calibrate the absolute power in our laser beam, we used the known self-focusing properties of CS_2, for which P_{cr} = 8kW. A 19 cm long CS_2 cell was inserted in place of the EBBA cell, and the radius at the exit plane of the sample was monitored using the techniques discussed above. Then using Eqs. (8), (9), and (10), the absolute value of $P(\zeta)$ was deter-

mined.

To calibrate the axial intensity monitored by D4, pinhole P1 was removed, and the signals from D4 and D2 were measured with laser pulses at least ten times below the self-focusing threshold. At the same time, photodiode D3 was calibrated by removing aperture A1 and allowing the specular reflections from the sample windows to enter D3.

Knowing the calibrations, we could determine the absolute stimulated Brillouin power generated in the backward direction for each laser shot. We could also determine the absolute axial intensity at the exit plane of the sample $I_{ax}(\zeta)$.

Then we could deduce the characteristic radius at the exit plane $r_o(\zeta)$ using

$$r_o^2(\zeta) = P_e(\zeta)/\pi\, I_{ax}(\zeta), \tag{15}$$

where the beam power at the exit plane is

$$P_e(\zeta) = P(\zeta) - P_{SBS}(\zeta). \tag{16}$$

Here Eq. (16) takes account of the depletion of the input power $P(\zeta)$ by the power fed into the Brillouin scattered beam $P_{SBS}(\zeta)$ if any. Eq. (15) will provide a useful characteristic radius unless the stimulated Brillouin scattering is so strong that it substantially changes the transverse profile of the beam. In our experiment, such substantial changes in the beam profile occured only at the very highest input powers used.

If the transverse profile of the beam is Gaussian, then from Eq. (15), we have

$$I(r,\zeta) = I_{ax}(\zeta)\, e^{-r^2/r_o^2(\zeta)} . \qquad (17)$$

In our analysis, we assumed the profile was Gaussian, and used Eq. (17) to compare our measurements of $I_{ax}(\zeta)$ to the streak photographs and the time-integrated photographs. We found good agreement, except for those cases having very strong stimulated Brillouin scattering. This was not surprising. It is known that the number of focal spots observed at the exit plane of a self-focusing sample is very sensitive to the spatial mode structure of the laser beam.[4,33] Because we consistently observed only one focal spot, we knew our beam must have a near Gaussian single transverse mode. Transient self-focusing experiments have shown that the focal spots have a near Gaussian profile around their center.[20,34] Calculations for both quasi-steady-state[3] and transient[21] self-focusing show that the off-axis parts of the beam should have more power than would be expected for a Gaussian profile. Thus Eq. (17) may overestimate the power near the axis, and underestimate the power far from the axis. Of course, it will be exactly correct for the power right on the axis.

D. Results

We made a series of measurements with different input laser powers for five values of t_p/τ listed in Table I. In Fig. 3, we present a typical set of results showing self-focusing for three clearly different cases: (I) near quasi-steady-state limit, $t_p/\tau = 11.3$; (II) the intermediate case, $t_p/\tau = 5.2$; and (III) near transient limit, $t_p/\tau = 0.21$. Figures 3(a) and 3(b) show respectively the input laser pulses $P(\zeta)$ and the axial intensity pulses $I_{ax}(\zeta)$, measured by the fast detectors D2 and D4 in Fig. 2. Each pulse is plotted with its leading edge at the right. Using Eq. (15) we could deduce the temporal variation of the beam radius $r_o(\zeta)$

at the end of the cell as shown in Fig. 3(d), and compared it directly with the observed streak camera picture in Fig. 3(e). We found the agreement in all cases was excellent. Note however that in the near quasi-steady-state case, only the leading part of the pulse can be seen because backward stimulated Brillouin scattering actually depletes the lagging part of the pulse and prevents it from self-focusing.

We present more extensive results showing $I_{ax}(\zeta)$ for a wide range of input laser powers in Fig. 4. For these same input powers, we show $r_o(\zeta)$ in Fig. 5 as determined from Eq. (15). Of all these shots, the peak of the axial intensity was substantially depleted by Brillouin scattering in only two shots, (c)(v) and (d)(v). This depletion caused Eq. (15) to give a minimum $r_o(\zeta)$ which was about 30% larger than the minimum $r_o(\zeta)$ which was deduced from the streak photograph. For these two shots only, the $r_o(\zeta)$ shown in Fig. 5 is deduced from the streak photograph rather than from Eq. (15). In Fig. 6 we show the corresponding streak photographs.

IV. DISCUSSION

A. Agreement with Theoretical Models

The radial profiles of the self-focused laser pulse in Fig. 3(c) can now be compared with those in Fig. 1. They clearly have the same qualitative features, which shows that our unified physical description in Fig. 1 is a valid description. In the transient limit the pulse had a horn shape with weak oscillations along the neck region, as predicted by the theory.[17,18] As t_p/τ was increased by decreasing τ, the axial intensity pulse decreased in length, and the radius started to diverge at the end of the pulse. In the quasi-steady-state limit ($t_p/\tau \gg 1$) the radius showed a localized focal spot, and the axial intensity pulse length was of the order of τ, in agreement with theoretical predictions.[11]

We can see the effect of varying input power in Fig. 5. The deformation of the longitudinal pulse profile is strikingly dependent on t_p/τ at all power levels investigated. As an example, let us examine the pulse deformation right at the self-focusing threshold. These low input power pulses are shown in Fig. 5(i). In the quasi-steady-state limit (see Fig. 5a(i)), the tail of the pulse was focused no more strongly than was the leading edge of the pulse. The peak of the pulse was focused most strongly, and $r_o(\zeta)$ was nearly symmetrical about $\zeta = 0$. As t_p/τ decreased (see Fig. 5b(i) and 5c(i)), the tail of the pulse was affected more and more by the onset of self-focusing. In the transient limit (see Fig. 5d(i)), the tail of the pulse was focused more strongly than any preceding part of the pulse. This behavior is in good agreement with the predictions of Fig. 1.

Another qualitative aspect of self-focusing one can deduce from Fig. 1 is that near the self-focusing threshold, the peak of the axial intensity pulse should be delayed from the peak of the input laser pulse if the transient effect is appreciable. For the transient cases, the self-focusing threshold is higher and the delay is longer. As the input power increases and the beam self-focuses more strongly, the peak of the axial intensity pulse will first move backward in time until the self-focused beam reaches its limiting diameter, and then it will move forward toward the peak of the input pulse. These features are what we actually observed in our experiment as shown in Fig. 7. For comparison, we include in Fig. 7 a theoretical curve (a) calculated using the quasi-steady-state formula Eq. (8) with the actual time dependence of the laser pulses we used in these measurements. The results in Fig. 7 indicate that even with $t_p/\tau = 11.3$, the transient effect on self-focusing is still quite appre-

ciable. For the more transient cases, the delay of the axial intensity pulse approached $\zeta_o \cong 0.3\ t_p$. This is in good agreement with the delay predicted in numerical calculations.[17,18]

In Fig. 8, we show the observed minimum radius of the self-focused beam at the end of the cell $R_{min} \equiv r_{o,min}/r_{o,input}$ as a function of the normalized input peak power P/P_{cr} for the various cases. The theoretical curve (a) for the quasi-steady-state limit is also plotted for comparison.[14] Curve (b) shows again that with $t_p/\tau = 11.3$, self-focusing is still somewhat transient. For the more transient cases, the minimum radius R_{min} of the self-focused beam shrank more gradually with increasing input power. Towards the transient limit, curves (e) and (f), R_{min} depended only on the quantity$(Pt_p/P_{cr}\tau)$, as predicted by theory.[18,19] Points of equal R_{min} on curves (e) and (f) occur at powers P/P_{cr} differing by a factor equal to the ratio of τ for the two curves. Curves (g) and (h) in Fig. 8 show the theoretical predictions for $t_p/\tau = 0.47$ and $t_p/\tau = 0.21$, based upon interpolation of the numerical results of Shimizu.[21] Presumably because of the onset of stimulated Brillouin scattering, our results deviate from the theoretical predictions as the limiting diameter is reached.

In Fig. 9, we show R_{min} as a function of P/P_{cr} for CS_2, which has a response time $\tau = 2$ sec. With $t_p/\tau = 7.5 \times 10^3$, this is the true quasi-steady-state limiting case. As expected, the solid theoretical curve for the quasi-steady-state limit agrees well with our experimental results down to the limiting value.

B. Limiting Mechanisms

In all cases, the R_{min} in Fig. 8 approached a limiting value at high P. As discussed in Section II, numerous mechanisms have been proposed

for this behavior. Here, let us estimate the effects of some of these mechanisms.

The limiting focal diameter could be due to saturation of Δn resulting from high degrees of molecular alignment in a Kerr liquid. In our experiments, however, we estimated the maximum Δn using Eqs. (5) and (15) and the measured axial intensities in Fig. 4. We found $\Delta n_{max} \cong .007$. For fully aligned EBBA with an order parameter of unity, Δn should be around 0.35. So, the maximum ordering in our sample is only 0.02. This is more than an order of magnitude less than the ordering present in the nematic phase, and is therefore far from saturation. From the known results on the optical field-induced refractive index in EBBA,[22] there should also be no steric or compressional effects[28] which could introduce saturation in Δn at our level of laser intensities.

Another possible mechanism of limiting the focal diameter is the generation of free electrons in pre-breakdown ionization.[29] This would require an electron density of $n \cong mc^2 I_{ax}/e^2 P_{cr}$ so that the plasma frequency is $\omega_p \approx \omega\left[n_o n_2 |E|^2\right]^{\frac{1}{2}}$. The total required number of free electrons for an appreciable reduction of Δn would then be $N \cong 5 \times 10^{13} P/P_{cr}$. From Fig. 8, we see that $N \cong 10^{15}$. However, our input pulse contained at most 5×10^{15} photons, and the quantum yield of photons into free electrons was certainly significantly less than 1. It could not create a sufficient electron density to reduce Δn appreciably unless virtually the whole beam were depleted. This means that any effect of pre-breakdown ionization would be from depletion of laser power rather than from its effect upon Δn. In our experiment, we did not see any evidence of depletion of the laser beam below the stimulated Brillouin scattering threshold. As a result the limiting value of R_{min} could not be due to laser depletion from

pre-breakdown ionization, or multiphoton absorption.

We have monitored in our experiment stimulated Raman and Brillouin scattering under all conditions. No stimulated Raman scattering was observed until the input power is substantially higher than the level at which the limiting diameter is reached. On the other hand, backward stimulated Brillouin scattering was always observed before the limiting diameter was reached. In Fig. 8, the stimulated Brillouin scattering threshold is marked by an arrow for each set of data. We see that in each case, the limiting value of R_{min} is reached at power slightly above the stimulated Brillouin threshold. We can therefore conclude that in our experiment stimulated Brillouin scattering must be the mechanism responsible for the limiting diameter.

Kelley and Gustafson[31] have pointed out that stimulated Brillouin scattering could not be the limiting mechanism in CS_2 or toluene because its response time was so much longer than the response time of Δn. In our experiment, the situation is different. We can estimate the acoustic response time in EBBA based upon measurements made on other organic liquids. For example, in toluene the response time is 0.3 nsec[35] and in a mixture of cholesteric liquid crystals, it is 0.6 nsec.[36] We infer that in EBBA, this response time should be less than 1 nsec. In our experiment, this means that the orientation relaxation time τ was always greater than the Brillouin response time. As a result, the Brillouin gain can more or less follow the variations of the self-focused laser beam intensity. Since the steady-state gain is higher for Brillouin scattering than for Raman scattering, we would expect Brillouin scattering to be dominant in our experiment.

In Fig. 8, we see that stimulated Brillouin scattering set in more

abruptly in the steady-state case, and thus stopped the shrinking beam radius more readily. For laser pulses well above the Brillouin threshold, we observed Brillouin depletion in excess of half of the beam power. Since the gain is highest on the beam axis, the most intense axial part of the beam was preferentially depleted, and Δn dropped along the beam axis. The light somewhat off the beam axis was much less depleted. So, Δn was higher off of the beam axis than it is on the axis. This should lead to a defocusing of the axial rays. A dynamic equilibrium was expected to set up: any tendency of the beam to further self-focus would result in an increased stimulated Brillouin scattering and the resulting additional depletion of laser power would oppose the tendency of the beam to further self-focus.

In Fig. 10, we show the variation of the peak Brillouin output power as a function of input power for the cases studied. Again, we see that the growth of the Brillouin power is clearly the most abrupt in the most steady-state case as expected.

V. CONCLUSION

Using the temperature dependence of the relaxation time τ in an isotropic liquid crystalline material, we have studied the variation of self-focusing from the quasi-steady-state to the transient limits. In all cases, our quantitative measurements of the time variation of the laser pulse radius strongly support the unified qualitative description of self-focusing in Fig. 1. We see that there is no abrupt change in the character of the self-focusing as t_p/τ is varied, but rather there is a smooth variation from one limit to the other. Our measurements are in good qualitative agreement with available theoretical predictions. Unfortunately, because numerical calculations of self-focusing for our cases do not ex-

ist at present, we have not yet been able to make quantitative comparison between theory and experiment over the entire range.

We acknowledge the use of facilities in the Materials and Molecular Research Division of Lawrence Berkeley Laboratory.

References

1. See, for example, Y. R. Shen, Prog. Quant. Elect. 4, 1 (1975); J. H. Marburger, Prog. Quant. Elect. 4, 35 (1975); O. Svelto, Prog. in Optics XII, 1 (1974); and S. A. Akhmanov, R. V. Khokhlov, and A. P. Sukhorukov, in Laser Handbook, p. 1151 edited by F. T. Arrechi and E. O. Schulz-Dubois, North-Holland Publishing Co. (1972).
2. V. N. Lugovoi and A. M. Prokhorov, Zh. Eksp. Teor. Fiz. Pis'ma 7, 153 (1968) (Translation: JETP Lett. 7, 117 (1968)); A. L. Dyshko, V. N. Lugovoi, and A. M. Prokhorov, Zh. Eksp. Teor. Fiz. Pis'ma 6, 665 (1967) (Translation: JETP Lett. 6, 146 (1967)); V. N. Lugovoi, Doklady Akad. Nauk SSSR 176, 58 (1967) (Translation: Sov. Phys. Doklady 12, 866 (1968)).
3. P. L. Kelley, Phys. Rev. Lett. 15, 1005 (1965); V. I. Talanov, Zh. ETF Pis'ma 2, 218 (1965) (Translation: JETP Lett. 2, 138 (1965)); S. A. Akhmanov, A. P. Sukhhorukov, and R. V. Khokhlov, Zh. Eksp. Teor. Fiz. 50, 1537 (1966) (Translation: Sov. Phys. JETP 23, 1025 (1966)).
4. M. M. T. Loy and Y. R. Shen, Phys. Rev. Lett. 22, 994 (1969).
5. M. M. T. Loy and Y. R. Shen, Phys. Rev. Lett. 25, 1333 (1970); M. M. T. Loy and Y. R. Shen, Appl. Phys. Lett. 19, 285 (1971).
6. V. V. Korobkin, A. M. Prokhorov, R. V. Serov, and M. Ya. Shchelev, Zh. ETF Pis'ma 11, 153 (1970) (Translation: JETP Lett. 11, 94 (1970)).
7. M. Maier, W. Kaiser, and J. A. Giordmaine, Phys. Rev. Lett. 17, 1275 (1966); Phys. Rev. 177, 580 (1969).
8. M. M. T. Loy and Y. R. Shen, IEEEJ Quant. Electron. QE-9, 409 (1973).
9. M. Maier, G. Wendl, and W. Kaiser, Phys. Rev. Lett. 24, 352 (1970); M. Maier, O. Rehn, and G. Wendl, Z. Naturforsh. A25, 1868 (1970).

10. G. K. L. Wong and Y. R. Shen, Appl. Phys. Lett. 21, 163 (1972).

11. Y. R. Shen and M. M. T. Loy, Phys. Rev. A3, 2099 (1971).

12. G. McAllister, J. Marburger, and L. De Shazer, Phys. Rev. Lett. 21, 1648 (1968).

13. V. N. Goldberg, V. I. Talanov, and R. E. Irm, Izv. Vysshikh. Uchebn. Zavedenii Radiofizika 10, 674 (1967).

14. J. H. Marburger and E. L. Dawes, Phys. Rev. Lett. 21, 556 (1968); E. L. Dawes and J. H. Marburger, Phys. Rev. 179, 862 (1969).

15. S. A. Akhmanov, A. P. Sukhorukov, and R. V. Khoklov, Zh. Eksp. Tech. Fiz. 51, 296 (1966) (Translation: JETP 24, 198 (1966)).

16. J. A. Fleck and P. L. Kelley, Appl. Phys. Lett. 15, 313 (1969).

17. J. A. Fleck and R. L. Carman, Appl. Phys. Lett. 20, 290 (1972).

18. F. Shimizu, IBM J. Res. Develop. 17, 286 (1973).

19. V. A. Aleshkevich, S. A. Akhmanov, A. P. Sukhorukov, and A. M. Khachatryan, Zh. ETF Pis'ma 13, 55 (1971) (Translation: JETP Lett. 13, 36 (1971)).

20. See, for example, R. Polloni, C. A. Sacchi, and O. Svelto, Phys. Rev. Lett. 23, 690 (1969); R. Cubeddu et al. Phys. Rev. Lett. 26, 1009 (1971).

21. G. K. L. Wong and Y. R. Shen, Phys. Rev. Lett. 32, 527 (1974).

22. G. K. L. Wong and Y. R. Shen, Phys. Rev. Lett. 30, 895 (1973); Phys. Rev. A10 1277 (1974).

23. E. G. Hanson, Y. R. Shen, and G. K. L. Wong, Phys. Rev. A14, 1281 (1976).

24. Y. R. Shen, Phys. Lett. 20, 378 (1966).

25. V. N. Goldberg, V. I. Talanov, and R. E. Irm, Izv. Vysshikh. Uchebn. Zavadenii Radiofizika 10, 674 (1967).

26. W. G. Wagner et al. Phys. Rev. 175, 256 (1968); J. H. Marburger et

al. Phys. Rev. 184, 255 (1969).

27. T. K. Gustafson et al. Appl. Phys. Lett. 12, 165 (1968); T. K. Gustafson et al. Phys. Rev. 177, 306 (1969).

28. T. K. Gustafson and C. H. Townes, Phys. Rev. A6, 1659 (1972).

29. E. Yablonovich and N. Bloembergen, Phys. Rev. Lett. 29, 907 (1972); N. Bloembergen, IEEEJ. Quant. Electr. QE-10, 375 (1974).

30. A. L. Dyshko, V. N. Lugovoi, and A. M. Prokhorov, Zh. Tekh. Fiz. 61, 2305 (1971) (Translation: Sov. Phys. JETP 34, 1235 (1972)).

31. P. L. Kelley and T. K. Gustafson, Phys. Rev. A8, 315 (1973).

32. O. Rehn and M. Maier, Phys. Rev. Lett. 29, 558 (1972); Phys. Rev. A9, 1427 (1974).

33. V. I. Bespalov and V. I. Talanov, Zh. ETF Pis'ma 3, 471 (1966) (Translation: JETP Lett. 3, 307 (1966)).

34. R. G. Brewer and C. H. Lee, Phys. Rev. Lett. 21, 267 (1968).

35. See, for example, Kaiser and Maier in Laser Handbook, vol. 2, p. 1077, edited by F. T. Arecchi and E. O. Schulz-Dobois, North-Holland (1972).

36. H. Rosen and Y. R. Shen, Mol. Cryst, and Liq. Cryst. 18, 285 (1972).

FIGURE CAPTIONS

Fig. 1. Schematic drawing showing how an imput pulse gets deformed through self-focusing (a) in the quasi-steady-state limit, (b) in an intermediate case, and (c) in the transient limit. Here the pulse is shown as viewed from the side in a series of snapshots.

Fig. 2. Experimental arrangement for observing self-focusing. B1, B2, B3, B4, B5, beamsplitters; L1, L2, L3, L4, L5, lenses; D1, D2, D3, D4, biplanar vacuum photodiodes; A1, aperature; P1, pinhole.

Fig. 3. Typical sets of results showing (a) input laser pulses, (b) on-axis intensity pulses, (c) radial profiles of the self-focused pulses, (d) intensity contours of the self-focused pulses, and (e) streak photographs. In each case the horizontal axis is the local time ξ. The intensity contour map shows the intensity as a function of transverse coordinate and time. Contours shown are $I = 0.30\ I_{max}$ and $I = 0.03\ I_{max}$. For $t_p/\tau = 11.3$, the input peak power is $P = 7.9$ kW, $P/P_{cr} = 5.5$, and the on-axis peak intensity is $I_{max} = 0.77\ GW/cm^2$. For $t_p/\tau = 5.2$: $P = 5.2$ kW, $P/P_{cr} = 5.6$, and $I_{max} = 0.75\ GW/cm^2$. For $t_p/\tau = 0.21$: $P = 4.4$ kW, $P/P_{cr} = 61$, and $I_{max} = 0.54\ GW/cm^2$.

Fig. 4. Axial intensity pulses.

(a) $t_p/\tau = 11.3$: (o) input pulse, (i) $P_o = 3.66$ kW, $I_{ax} = 38\ MW/cm^2$ (ii) $P_o = 4.42$ kW, $I_{ax} = 75.5\ MW/cm^2$ (iii) $P_o = 5.17$ kW, $I_{ax} = 431\ MW/cm^2$ (iv) $P_o = 7.86$ kW, $I_{ax} = 768\ MW/cm^2$ (v) $P_o = 9.18$ kW, $I_{ax} = 705\ MW/cm^2$

(b) t_p/τ = 5.2: (o) input pulse,			(i) P_o = 2.58 kW, I_{ax} = 28.8 MW/cm^2		
(ii) P_o =	3.58	89.7	(iii)	4.07	304
(iv)	5.17	753	(v)	6.15	864
(c) t_p/τ = 2.07:			(i)	1.21	8.0
(ii)	2.27	3.52	(iii)	3.65	481
(iv)	4.33	560	(v)	6.80	348
(d) t_p/τ = 0.21:			(i)	0.99	6.4
(ii)	1.93	102	(iii)	2.44	150
(iv)	4.35	544	(v)	7.41	538

Fig. 5. Pulse radius at exit plane of cell, for the same pulses as in Fig. 4.

Fig. 6. Streak photographs, for the same pulses as in Fig. 4.

Fig. 7. Peak position of the on-axis intensity pulse of the self-focused beam as a function of normalized input peak power in different cases: (a) $t_p/\tau \to \infty$, (a theoretical curve), (b) t_p/τ = 11.3, (c) t_p/τ = 5.2, (d) t_p/τ = 2.07, and (e) t_p/τ = 0.47. Curve (a) is calculated from Eq. (8), which gives z_f = 10 cm for P = 2.97 P_{cr}.

Fig. 8. Reduced minimum radius of the self-focused beam at the end of the cell as a function of normalized input peak power in various cases: (a) $t_p/\tau \to \infty$ (a theoretical curve from Ref. 13), (b) t_p/τ = 11.3, (c) t_p/τ = 5.2, (d) t_p/τ = 2.07, (e) t_p/τ = 0.47, (f) t_p/τ = 0.21, (g) t_p/τ = 0.47 (a theoretical curve from Ref. 21), and (h) t_p/τ = 0.21 (a theoretical curve from ref. 21).

Fig. 9. Reduced minimum radius of the self-focused beam at the end of the cell as a function of normalized input peak power for CS_2. Here the solid curve is calculated from Eqs. (8), (10), and (13)

using z = 19 cm.

Fig. 10. Peak output power of the backward stimulated Brillouin pulse, as a function of the normalized input power in the various cases studied.

TABLE CAPTIONS

Table I Characteristic parameters of EBBA (T_K = 78°) used as a self-focusing medium, with laser pulses having a full width at half maximum t_p = 15 nsec.

TABLE I

T (°C)	τ nsec	t_p/τ	n_2 (10^{-11} esu)	P_{cr} (kW)
79.7	72.5	0.21	237	0.071
82.7	32.1	0.47	111	0.151
96.0	7.25	2.07	33.4	0.503
112.0	2.87	5.2	18.2	0.926
130.8	1.33	11.3	11.8	1.420

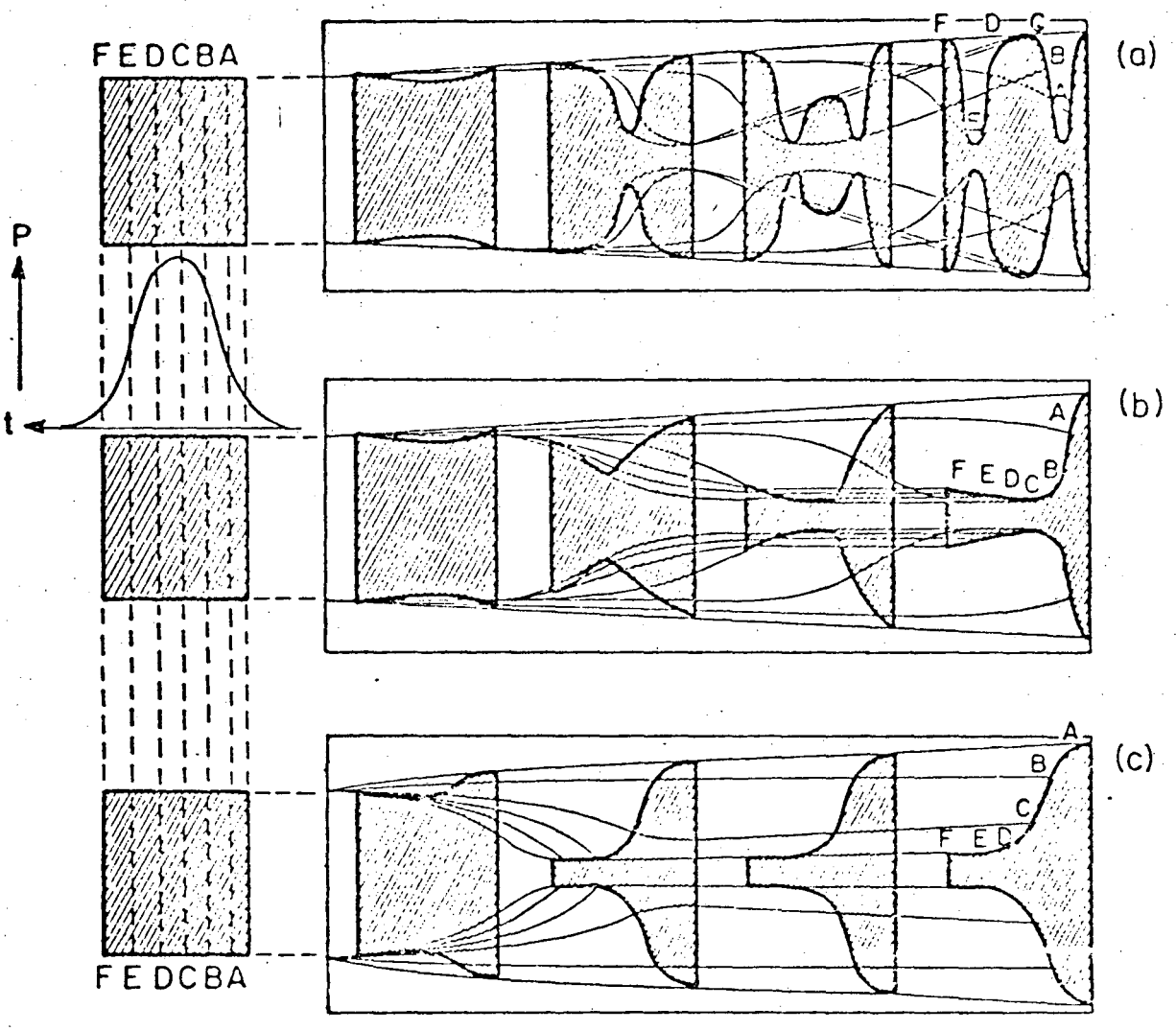

XBL 765-6830

Fig. 1

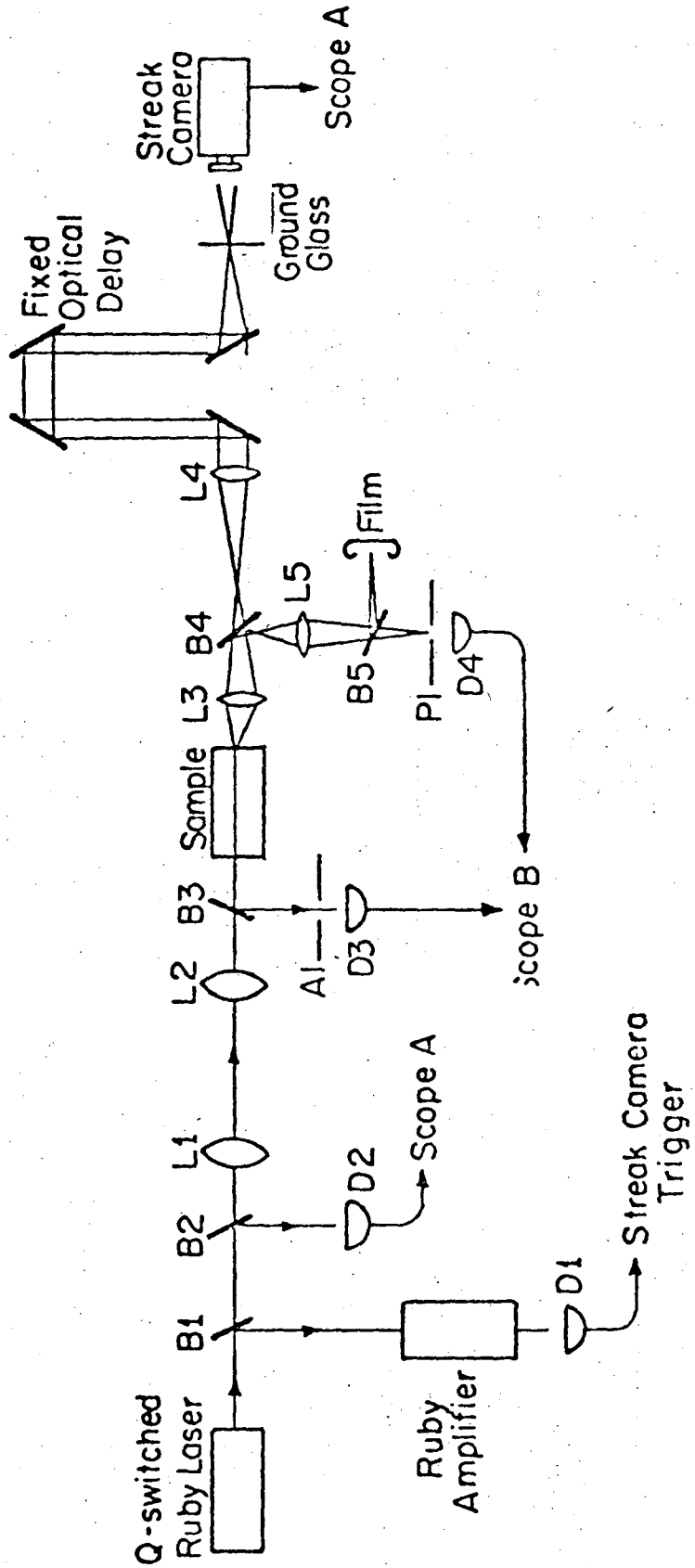

XBL 765-6831

Fig. 2

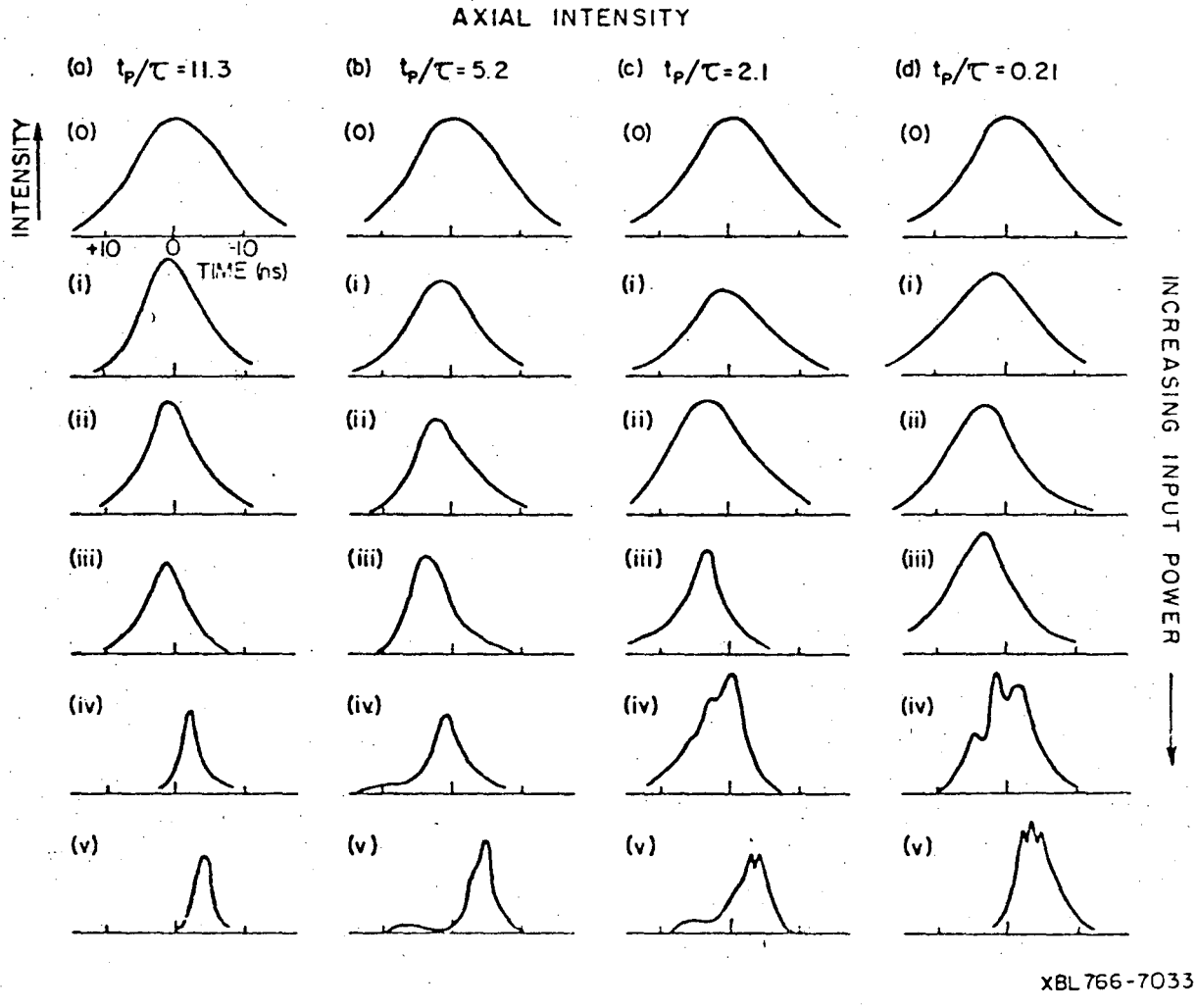

Fig. 4

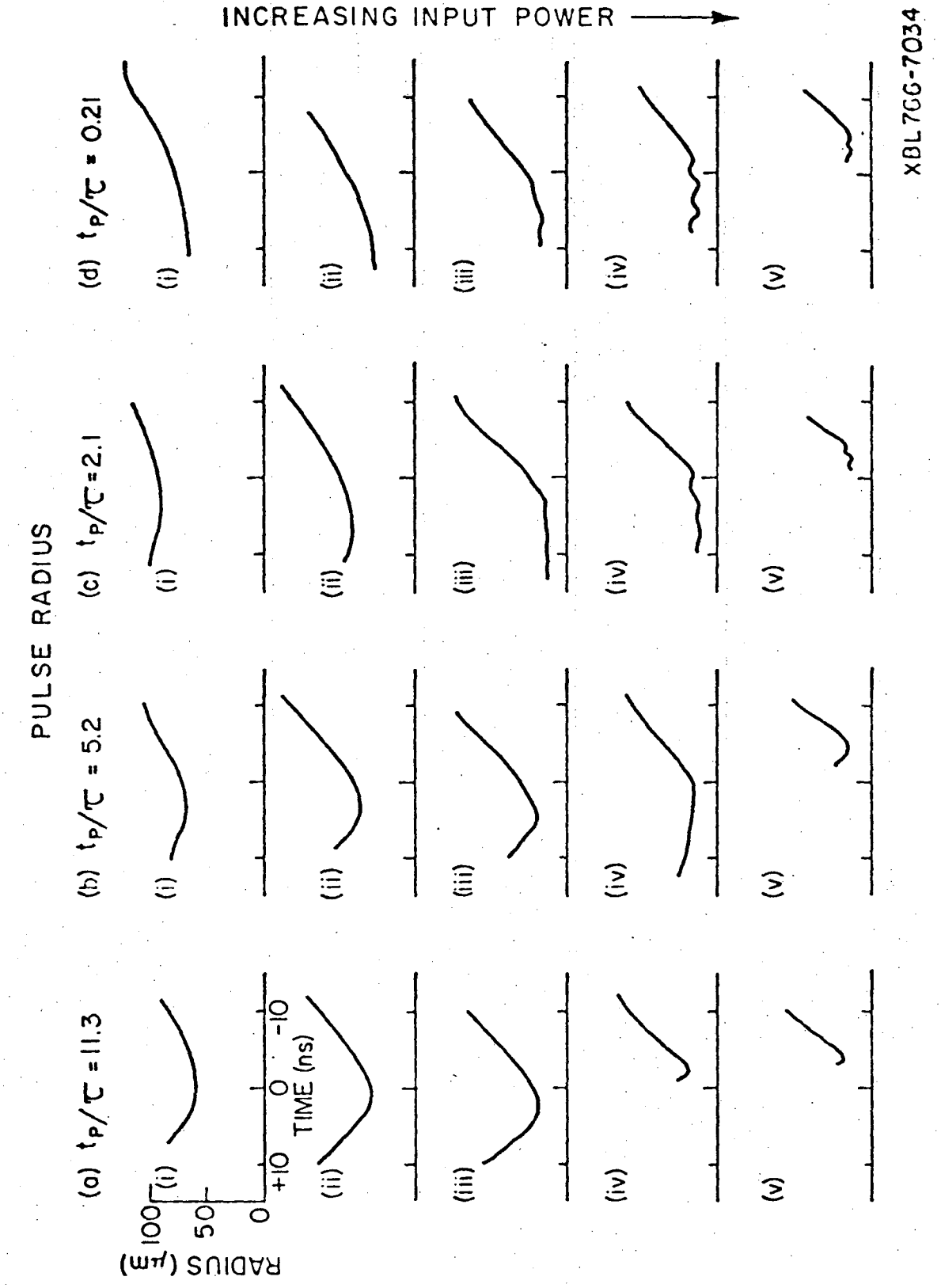

Fig. 5

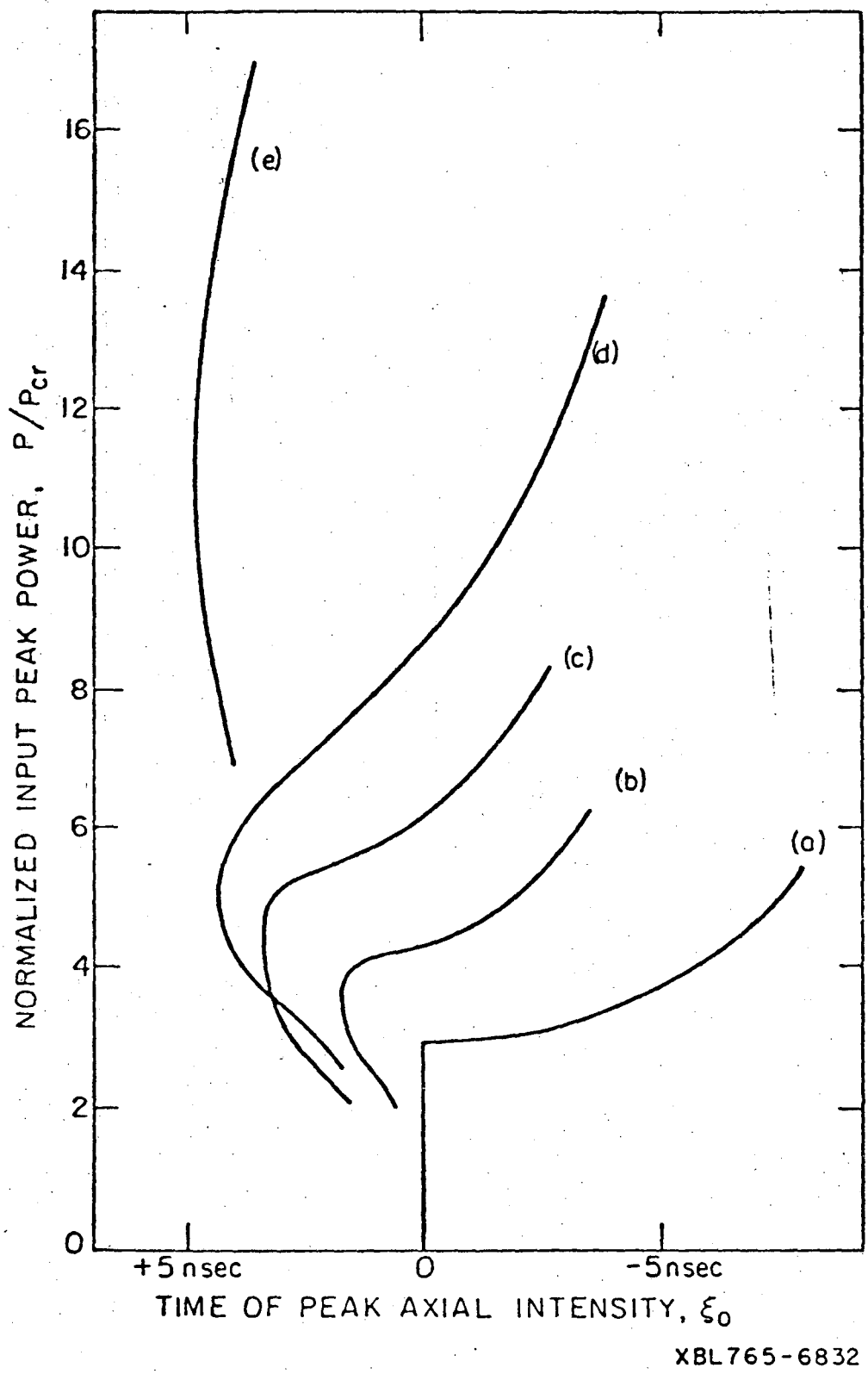

Fig. 7

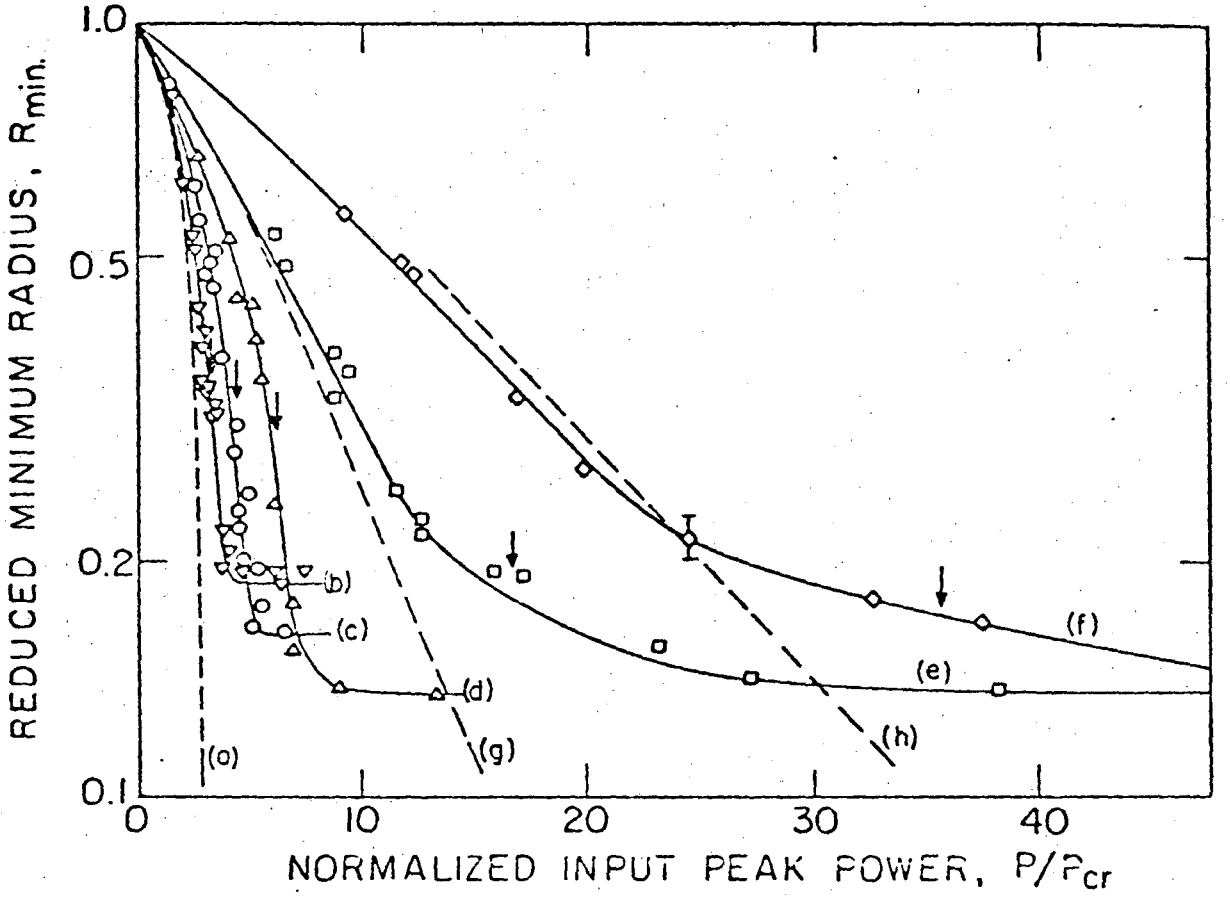

XBL 766-7031

Fig. 3

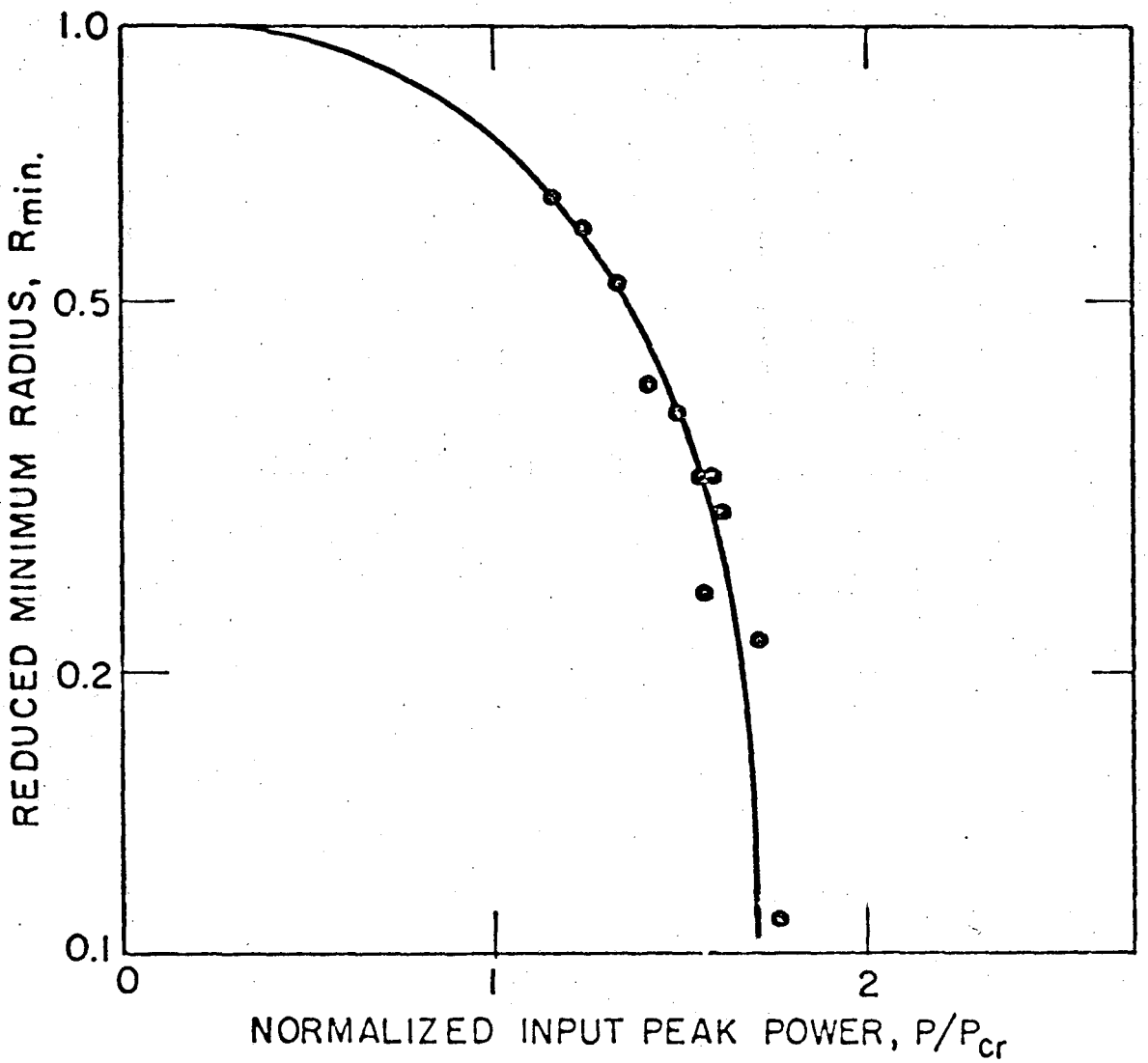

XBL 7612-11,468

Fig. 9

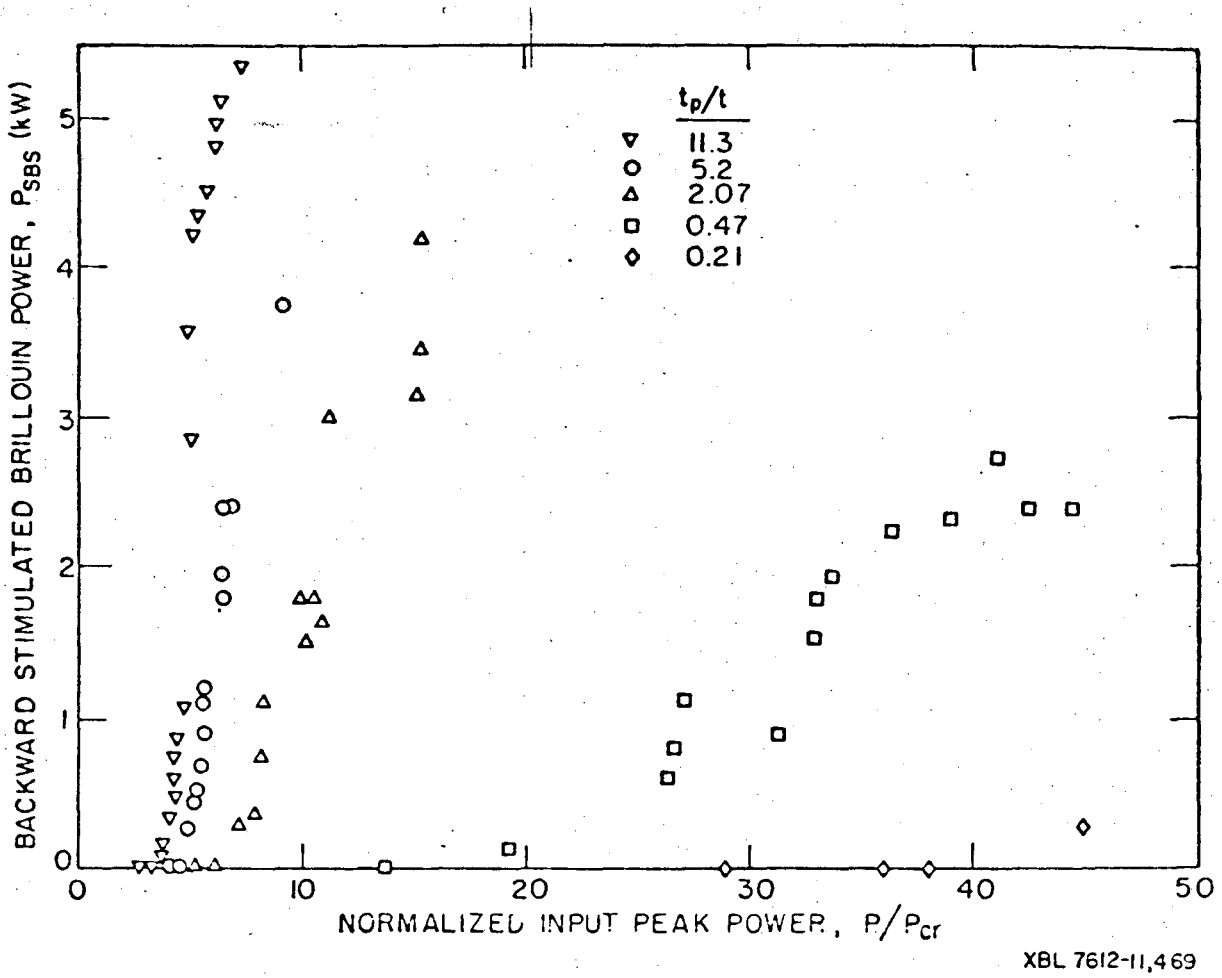

Fig. 10

This report was done with support from the United States Energy Research and Development Administration. Any conclusions or opinions expressed in this report represent solely those of the author(s) and not necessarily those of The Regents of the University of California, the Lawrence Berkeley Laboratory or the United States Energy Research and Development Administration.

TECHNICAL INFORMATION DIVISION
LAWRENCE BERKELEY LABORATORY
UNIVERSITY OF CALIFORNIA
BERKELEY, CALIFORNIA 94720